Electromagnetic bremsstrahlung and energy loss in chiral medium

Jeremy Hansen and Kirill Tuchin◉

Department of Physics and Astronomy, Iowa State University, Ames, Iowa 50011, USA

We study electromagnetic radiation by a fast particle carrying electric charge in chiral medium. The medium is homogeneous and isotropic and supports the chiral magnetic current which renders the fermion and photon states unstable. The instability manifests as the chirality-dependent resonances in the bremsstrahlung cross section, which enhance the energy loss in the chiral medium. We compute the corresponding cross sections in the single scattering approximation and derive the energy loss in the high-energy approximation.

I. INTRODUCTION

This paper is the third in the series of papers dedicated to the problem of energy loss by a fast particle in the chiral medium due to the electromagnetic interactions. The pivotal feature of chiral media is the peculiar response to the external electromagnetic field caused by the chiral anomaly [1,2]. In homogeneous media, it is given by the chiral magnetic current $\boldsymbol{j} = b_0 \boldsymbol{B}$ [3–7], where the chiral magnetic conductivity b_0 is assumed to be a constant. It was discussed in the context of Weyl and Dirac semimetals [8–10], the quark-gluon plasma [11,12] and the axion phenomenology [13]. In our first paper [14] we computed the collisional energy loss and found that at high energies it is dominated by the chiral Cherenkov radiation. In the second paper [15] we considered the part of the radiative energy loss that is driven by the resonance at $\boldsymbol{q}^2 = b_0^2$ in the spatial part of the photon propagator $D_{ij}(q)$. The corresponding contribution to the bremsstrahlung cross section is proportional to the magnetic moment of the scatterer because D_{ij} couple only to the spatial part of the source current whose leading multipole term is the magnetic moment $\mathbb{M}$. It will be further referred to as the "magnetic channel". The emergence of the resonance is a signature of the chiral magnetic instability [16–18]. Another manifestation of this instability is the appearance of the chiral run-away modes in the modified photon dispersion relation. At high energies the anomalous term in the photon dispersion relation is small and can be neglected compared to the main contribution stemming from the pole in D_{ij}. This is to say that the

resonance in the magnetic bremsstrahlung cross section is weakly dependent on the radiated photon kinematics.

In this article we consider the photon bremsstrahlung in the chiral medium due to the Coulomb part $D_{00}(q)$ of the photon propagator. We dub it the "electric channel". Although $D_{00}(q)$ itself has no conspicuous dependence on b_0, the resonance does emerge in the photon propagator due to the anomaly in the photon dispersion relation. It causes the momentum transfer $\boldsymbol{q}^2$ to vanish at finite photon emission angles θ. Thus, unlike the magnetic channel considered in [15], the electric channel is driven exclusively by the anomaly in the photon dispersion relation. Along with the photon propagator, the fermion one also becomes resonant, indicating instability of fermions in the chiral medium [17,18]. The main goal of this paper is to compute the photon bremsstrahlung cross section in the chiral medium due to the Coulomb term in the photon propagator.

The paper is structured as follows. In Sec. II we derive the general expression for the scattering cross section. In Sec. III we observe that the cross section is divergent due to the resonances in the photon and fermion propagators. The divergences are regulated by the finite width of the unstable modes which is proportional to the fermion relaxation rate τ^{-1}. Significantly, the same parameter regulates the divergences in the fermion and photon propagators in the electric channel (but not in the magnetic one discussed in [15]). The final expression for the scattering cross section is quite bulky and is given in Appendix A. The high-energy limit, relevant in most applications, is developed in Sec. IV where the resonant structures become very clear. Particularly simple expressions for the cross section are derived at low and high temperatures. Our main results are Eqs. (26), (28), (34), and (35) for the bremsstrahlung cross section in various limits. The results for the corresponding energy loss are given in Sec. V. The summary and outlook are presented in Sec. VI.

II. SCATTERING CROSS SECTION

Following the original Bethe and Heitler calculation [19], we consider scattering of a charged fermion off a heavy nucleus of mass M, electric charge eZ and magnetic moment $\mathbb{M}$. The differential cross section for photon radiation is given by the familiar expression

$$d\sigma = \frac{1}{2}\sum_{ss'\lambda}|\mathcal{M}|^2 \frac{1}{8(2\pi)^5}\frac{\omega|\boldsymbol{p}'|}{|\boldsymbol{p}|}d\Omega_k d\Omega' d\omega, \qquad (1)$$

where $p = (E, \boldsymbol{p})$, $p' = (E', \boldsymbol{p}')$ and $k = (\omega, \boldsymbol{k})$ are the incoming fermion, outgoing fermion, and radiated photon momenta respectively. The matrix element $\mathcal{M}$ is represented by two Feynman diagrams shown in Fig. 1. The corresponding analytical expression reads,

$$\mathcal{M} = e^2 \bar{u}(p')\left(\not{e}_{k\lambda}^* \frac{\not{p}' + \not{k} + m}{2p'\cdot k + k^2}\not{A}(\boldsymbol{q})\right.$$
$$\left. - \not{A}(\boldsymbol{q})\frac{\not{p} - \not{k} + m}{2p\cdot k - k^2}\not{e}_{k\lambda}^*\right)u(p), \qquad (2)$$

where $A(\boldsymbol{q})$ indicates the external field, $q = p' - p + k$ is the momentum transfer, m is the mass of the fermion, and $e_{k\lambda}$ is the photon polarization vector. Whereas in vacuum the photon four-momentum is lightlike, in chiral media it is not. Moreover, in the Lorentz gauge, photon is forced to be in one of the two circularly polarized states. This eliminates the residual gauge invariance that is reflected in the Ward identity [15]. The photon dispersion relation is

$$\omega^2 = \boldsymbol{k}^2 + k^2 = \boldsymbol{k}^2 - \lambda b_0|\boldsymbol{k}|, \qquad (3)$$

where $\lambda = \pm 1$ is right- or left-photon polarization.

The electromagnetic potential induced by the electric current J^μ, associated with the nucleus, in a chiral medium is $A_\mu = -iD_{\mu\nu}J^\nu$. The photon propagator in chiral medium in the Lorentz/Landau gauge takes the form [15],
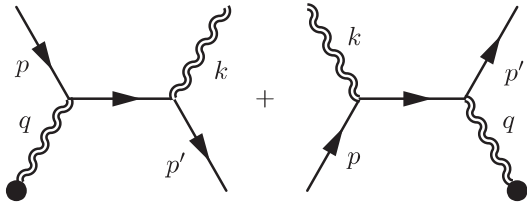

FIG. 1. The two diagrams corresponding to the matrix element for the scattering cross section. Double lines indicate photons in chiral medium.

$$D_{\mu\nu}(q) = -i\frac{q^2 g_{\mu\nu} + i\epsilon_{\mu\nu\rho\sigma}b^\rho q^\sigma + b_\mu b_\nu}{q^4 + b^2 q^2 - (b\cdot q)^2}$$
$$+ i\frac{[q^2 - (b\cdot q)^2/q^2]q_\mu q_\nu + b\cdot q(b_\mu q_\nu + b_\nu q_\mu)}{q^2[q^4 + b^2 q^2 - (b\cdot q)^2]}, \qquad (4)$$

where $b_\mu = (b_0, \boldsymbol{0})$. In the static limit $q^0 = 0$ the components of the photon propagator read [20]

$$D_{00}(\boldsymbol{q}) = \frac{i}{\boldsymbol{q}^2}, \qquad (5a)$$

$$D_{0i}(\boldsymbol{q}) = D_{i0}(\boldsymbol{q}) = 0, \qquad (5b)$$

$$D_{ij}(\boldsymbol{q}) = -\frac{i\delta_{ij}}{\boldsymbol{q}^2 - b_0^2} - \frac{\epsilon_{ijk}q^k}{b_0(\boldsymbol{q}^2 - b_0^2)} + \frac{\epsilon_{ijk}q^k}{b_0\boldsymbol{q}^2} + \frac{iq_i q_j}{\boldsymbol{q}^2(\boldsymbol{q}^2 - b_0^2)}. \qquad (5c)$$

The gauge-dependent terms proportional to q_μ and q_ν vanish when substituted into the scattering amplitude. The spatial components [Eq. (5)] couple to the nucleus magnetic moment and have a resonance at $\boldsymbol{q}^2 = b_0^2$. We analyzed this magnetic channel in our previous paper [15]. In this paper we are interested in the monopole component of the external field which is determined by the nuclear electric charge. Convolution of the current $J^\nu(\boldsymbol{x}) = eZ\delta^\nu{}_0\delta(\boldsymbol{x})$ with the D_{00} component of the photon propagator gives rise to the Coulomb potential,

$$A^0(\boldsymbol{q}) = eZ/\boldsymbol{q}^2, \qquad \boldsymbol{A}(\boldsymbol{q}) = 0. \qquad (6)$$

Plugging (6) into (2) and averaging over the fermion spin directions, we can obtain a fairly compact expression for the differential cross section of the electric channel,

$$d\sigma = \frac{Z^2}{2}\sum_\lambda \frac{d\Omega_k d\Omega' d\omega}{4(2\pi)^5}\frac{|\boldsymbol{p}'|}{|\boldsymbol{p}|}\frac{e^6}{\omega\boldsymbol{q}^4}\left\{4\left|\frac{Ep'\cdot e_\lambda}{\kappa' + \frac{k^2}{2\omega}} - \frac{E'p\cdot e_\lambda}{\kappa - \frac{k^2}{2\omega}}\right|^2\right.$$
$$- \boldsymbol{q}^2\left|\frac{p'\cdot e_\lambda}{\kappa' + \frac{k^2}{2\omega}} - \frac{p\cdot e_\lambda}{\kappa - \frac{k^2}{2\omega}}\right|^2 + \frac{\omega^2(\boldsymbol{q}^2 - (\kappa - \kappa' - \frac{k^2}{\omega})^2)}{(\kappa - \frac{k^2}{2\omega})(\kappa' + \frac{k^2}{2\omega})}$$
$$+ \frac{k^2}{4}\left[\boldsymbol{q}^2\left(\frac{1}{\kappa - \frac{k^2}{2\omega}} - \frac{1}{\kappa' + \frac{k^2}{2\omega}}\right)^2 + \frac{4|p\cdot e_\lambda - p'\cdot e_\lambda|^2}{(\kappa - \frac{k^2}{2\omega})(\kappa' + \frac{k^2}{2\omega})}\right.$$
$$\left.\left. - 4\left(\frac{E'}{\kappa - \frac{k^2}{2\omega}} - \frac{E}{\kappa' + \frac{k^2}{2\omega}}\right)^2\right]\right\}, \qquad (7)$$

where $\kappa = p\cdot k/\omega$ and $\kappa' = p'\cdot k/\omega$. In (7) the sum over λ is left explicit in order to isolate individual photon polarizations. Equation (7) reduces to the Bether-Heitler formula in the limit $|\boldsymbol{k}| \to \omega$, or, equivalently, $k^2 \to 0$.

The photon plane waves can only have a circular polarization which satisfies the transversality condition

$k \cdot e_k = \boldsymbol{k} \cdot \boldsymbol{e}_\lambda = 0$ in the Lorentz gauge. We seek computing the cross section for each photon polarization. To perform the angular integrals in (7) it is advantageous to eliminate the photon-polarization vectors in favor of particle momenta. To this end, we introduce a Cartesian reference frame with the z-axis pointing in the direction of the photon momentum $\boldsymbol{k}$,

$$\boldsymbol{k} = (0, 0, |\boldsymbol{k}|), \qquad \boldsymbol{e}_\lambda = \frac{1}{\sqrt{2}}(1, i\lambda, 0),$$

$$\boldsymbol{p} = (p_\perp, 0, p_\parallel), \qquad \boldsymbol{p}' = (p'_\perp \cos\phi, p'_\perp \sin\phi, p'_\parallel), \qquad (8)$$

where ϕ is the azimuthal angle. We derive the following identities:

$$|\boldsymbol{p} \cdot \boldsymbol{e}_\lambda|^2 = \frac{|\boldsymbol{p} \times \boldsymbol{k}|^2}{2\boldsymbol{k}^2}, \qquad (9a)$$

$$|\boldsymbol{p}' \cdot \boldsymbol{e}_\lambda|^2 = \frac{|\boldsymbol{p}' \times \boldsymbol{k}|^2(\cos^2\phi + \lambda^2\sin^2\phi)}{2\boldsymbol{k}^2} = \frac{|\boldsymbol{p}' \times \boldsymbol{k}|^2}{2\boldsymbol{k}^2}, \qquad (9b)$$

$$(\boldsymbol{p} \cdot \boldsymbol{e}_\lambda)(\boldsymbol{p}' \cdot \boldsymbol{e}_\lambda^*) = \frac{|\boldsymbol{p} \times \boldsymbol{k}||\boldsymbol{p}' \times \boldsymbol{k}|(\cos\phi - i\lambda \sin\phi)}{2\boldsymbol{k}^2}, \qquad (9c)$$

$$\boldsymbol{q}^2 = \boldsymbol{p}^2 + \boldsymbol{p}'^2 + \boldsymbol{k}^2 + 2\boldsymbol{k} \cdot \boldsymbol{p}' - 2\boldsymbol{k} \cdot \boldsymbol{p}$$
$$- 2\frac{\boldsymbol{k} \cdot \boldsymbol{p}\,\boldsymbol{k} \cdot \boldsymbol{p}' + |\boldsymbol{k} \times \boldsymbol{p}||\boldsymbol{k} \times \boldsymbol{p}'| \cos\phi}{\boldsymbol{k}^2}. \qquad (9d)$$

We observe that the dependence on the azimuthal angle ϕ appears in (7) only by the way of (9c) and (9d). Therefore, all terms proportional to $\sin\phi$ in (7) vanish after integration over the directions of the outgoing fermion. This conclusion holds even after we regulate the divergence in the fermion propagator using (13) in the next section. Dropping the imaginary part of $(\boldsymbol{p} \cdot \boldsymbol{e}_\lambda)(\boldsymbol{p}' \cdot \boldsymbol{e}_\lambda^*)$, observing that

$$p \cdot p' = m^2 + \omega(\kappa' - \kappa) + \frac{k^2 - q^2}{2}, \qquad (10)$$

and using (8), the nonvanishing terms proportional to $e_\lambda^i e_\lambda^{*j}$ can be written in terms of κ, κ' and q^2,

$$|\boldsymbol{e}_\lambda \cdot \boldsymbol{p}|^2 = \frac{|\boldsymbol{k} \times \boldsymbol{p}|^2}{2\boldsymbol{k}^2} = \frac{\boldsymbol{p}^2}{2} - \frac{(\boldsymbol{p} \cdot \boldsymbol{k})^2}{2\boldsymbol{k}^2} = \frac{\omega^2 E\kappa}{\boldsymbol{k}^2} - \frac{k^2}{2\boldsymbol{k}^2}E^2$$
$$- \frac{m^2}{2} - \frac{\omega^2}{2\boldsymbol{k}^2}\kappa^2, \qquad (11a)$$

$$|\boldsymbol{e}_\lambda \cdot \boldsymbol{p}'|^2 = \frac{\omega^2 E'\kappa'}{\boldsymbol{k}^2} - \frac{k^2}{2\boldsymbol{k}^2}E'^2 - \frac{m^2}{2} - \frac{\omega^2}{2\boldsymbol{k}^2}\kappa'^2, \qquad (11b)$$

$$\mathrm{Re}[(\boldsymbol{e}_\lambda \cdot \boldsymbol{p})(\boldsymbol{e}_\lambda^* \cdot \boldsymbol{p}')] = \frac{\boldsymbol{p} \cdot \boldsymbol{p}'}{2} - \frac{(\boldsymbol{p} \cdot \boldsymbol{k})(\boldsymbol{p}' \cdot \boldsymbol{k})}{2\boldsymbol{k}^2}$$
$$= \frac{\omega^2(\kappa'E' + \kappa E - \kappa\kappa') - \omega k^2(\kappa - \kappa') - k^2 EE'}{2\boldsymbol{k}^2} - \frac{m^2}{2} - \frac{k^2 + q^2}{4}. \qquad (11c)$$

Equations (11) can then be used to rewrite (7) without an explicit dependence on the photon-polarization vectors.

III. REGULATION OF THE RESONANCES

An examination of the fermion and photon propagators used in the calculation of the differential cross section reveals divergences in three kinematic regions: $q^2 = 0$, $2\omega\kappa = k^2$ and $2\omega\kappa' = -k^2$. The first one is the familiar infrared Coulomb pole $q^2 = 0$ which is regulated in the usual way [22,23],

$$\frac{1}{q^2} \to \frac{1}{q^2 + \mu^2}, \qquad (12)$$

where μ is the Debye mass of the medium. If the scattering particle mass m is much larger than μ, the minimum momentum transfer is of the order m. However, the

Debye mass scales with the temperature and becomes much larger than m in a sufficiently hot medium.[1] Therefore, in the following analysis it will be convenient to consider two limiting cases depending on the relative magnitude of m and μ. In the next section we will revisit the behavior of the photon propagator at small momentum transfers and show that due to the anomaly, q^2 can vanish at finite m. We will revise the regularization procedure accordingly.

The other two divergences occur in the fermion propagator and reflect its instability in chiral matter with respect to spontaneous photon emission [16,18,24–39]. With the account of the finite width the fermion propagators in (7) are modified as follows:

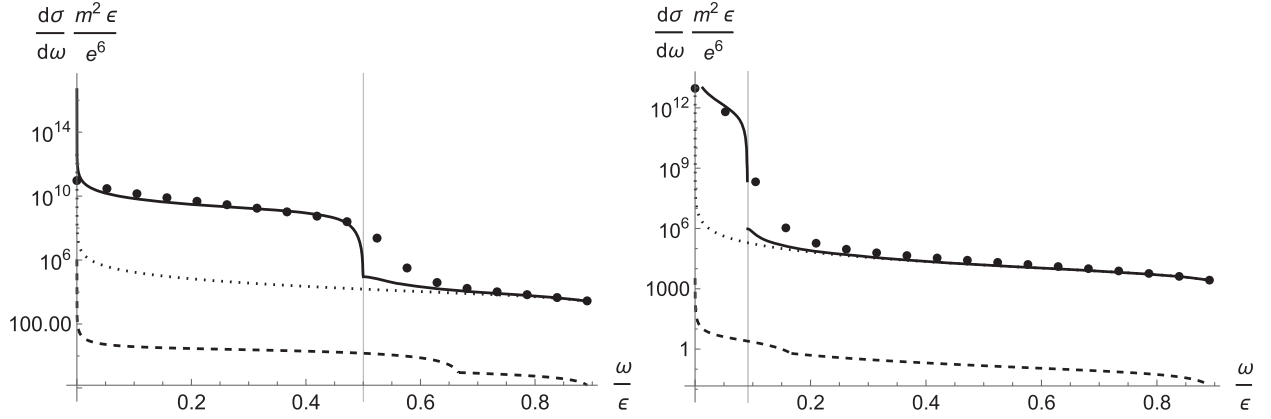[1]In hot plasmas the long-distance terms neglected in (12), see e.g., [21], may become important.

FIG. 2. The bremsstrahlung spectrum at $\mu \ll m$. The dots represent the exact leading order formula (A1), the solid line is the high-energy approximation given by the sum of Eqs. (26) and (28), the dotted line is the Bethe-Heitler expression (27), and the dashed line is the magnetic moment contribution (30). Left panel: $b_0 = 0.1m$, $\mu = 10^{-3}b_0$, $\tau^{-1} = 0.1b_0$. Right panel: $b_0 = 10^{-2}m$, $\mu = 10^{-3}b_0$, $\tau^{-1} = 0.1b_0$. Both panels: $E = 10m$, $Z = 33$, $\mathbb{M} = \mu_N$, $\Gamma = 0.1b_0$. The vertical line indicates ω^*/E.

$$
\frac{1}{2\omega\kappa - k^2} \to \frac{1}{2\omega\kappa - k^2 + iE/\tau},
$$
$$
\frac{1}{2\omega\kappa' + k^2} \to \frac{1}{2\omega\kappa' + k^2 - iE'/\tau}, \tag{13}
$$

where τ is the relaxation time as measured in the medium rest frame.[2] A number of inelastic processes contribute to the relaxation of the chiral state of the fermion. Among them is the spontaneous photon emission, also known in the literature as the vacuum or chiral Cherenkov radiation. Its rate at the leading order in the perturbation theory is

$$
W = \frac{e^2}{8\pi} \int \frac{d\omega}{\omega} \left[b_0 \left(\frac{\omega^2}{2E^2} - \frac{\omega}{E} + 1 \right) - \frac{m^2\omega}{E^2} \right] \Theta(\omega^* - \omega) \Theta(\lambda b_0), \tag{14}
$$

where the threshold photon energy is

$$
\omega^* = \frac{\lambda b_0 E^2}{\lambda b_0 E + m^2} \tag{15}
$$

and Θ is the step function [18]. In particular, when $m^2 \gg \lambda b_0 E$, the fermion decay rate is $W \approx \alpha b_0/2$. One can take this as the low bound of the total relaxation rate; $\tau^{-1} > \alpha b_0/2$.

We now have all necessary ingredients to complete our calculation of the differential cross section. Equation (7) may be integrated over directions term by term while making the substitutions (13) and (12) in order to obtain the frequency dependence of the differential cross section. The result is given by (A1) and (A2) in Appendix A. We use it for the numerical calculation presented in Fig. 2.

_____

[2]In the fermion rest frame the relaxation rate is $(E/m)\tau^{-1}$.

IV. HIGH-ENERGY LIMIT

The exact expression for the cross section (A1) is rather complicated. In applications one is usually interested in the high-energy limit $E, E' \gg m$, μ where the expression for the differential cross section and squared matrix element significantly simplify. To derive the high-energy limit, it is convenient to expand the squared amplitude before the integration over the fermion directions,

$$
\frac{1}{2}\sum_{s,s'}|\mathcal{M}|^2 \approx \frac{2Z^2e^6}{\omega^2(q^2+\mu^2)^2}\mathrm{Re}\left[4\left| \frac{Ep'\cdot e_\lambda}{\kappa'+\frac{k^2}{2\omega}+i\frac{E'}{\tau\omega}} - \frac{E'p\cdot e_\lambda}{\kappa-\frac{k^2}{2\omega}+i\frac{E}{\tau\omega}} \right|^2 \right.
$$
$$
+\frac{\omega^2(q^2-(\kappa-\kappa'-\frac{k^2}{\omega})^2)}{(\kappa-\frac{k^2}{2\omega}+i\frac{E}{\tau\omega})(\kappa'+\frac{k^2}{2\omega}-i\frac{E'}{\tau\omega})}
$$
$$
+k^2\left(\frac{q^2}{4}\left| \frac{1}{\kappa-\frac{k^2}{2\omega}+i\frac{E}{\tau\omega}} - \frac{1}{\kappa'+\frac{k^2}{2\omega}+i\frac{E'}{\tau\omega}} \right|^2 \right.
$$
$$
+\frac{|p\cdot e_\lambda - p'\cdot e_\lambda|^2}{(\kappa-\frac{k^2}{2\omega}+i\frac{E}{\tau\omega})(\kappa'+\frac{k^2}{2\omega}-i\frac{E'}{\tau\omega})}
$$
$$
\left.\left. -\left| \frac{E'}{\kappa-\frac{k^2}{2\omega}+i\frac{E}{\tau\omega}} - \frac{E}{\kappa'+\frac{k^2}{2\omega}+i\frac{E'}{\tau\omega}} \right|^2 \right) \right]. \tag{16}
$$

Additionally, we are interested in photon energies $\omega \gg b_0$ which allows us to write the dispersion relation (3) as

$$
|\boldsymbol{k}| \approx \omega + \frac{\lambda b_0}{2}, \tag{17}
$$

and treat $k^2/\omega^2 \approx -\lambda b_0/\omega$ as a small parameter. In this limit Eq. (11) may be rewritten as

$$|e_\lambda \cdot \boldsymbol{p}|^2 \approx \left(1 - \lambda \frac{b_0}{\omega}\right)^2 E\kappa + \left(\frac{\lambda b_0}{2\omega} - \frac{b_0^2}{2\omega^2}\right) E^2$$
$$- \frac{m^2 + (1 - \lambda \frac{b_0}{\omega})^2 \kappa^2}{2}, \tag{18a}$$

$$|e_\lambda \cdot \boldsymbol{p}'|^2 \approx \left(1 - \lambda \frac{b_0}{\omega}\right)^2 E'\kappa' + \left(\frac{\lambda b_0}{2\omega} - \frac{b_0^2}{2\omega^2}\right) E'^2$$
$$- \frac{m^2 + (1 - \lambda \frac{b_0}{\omega})^2 \kappa'^2}{2}, \tag{18b}$$

$$\mathrm{Re}[(e_\lambda \cdot \boldsymbol{p})(e_\lambda^* \cdot \boldsymbol{p}')] = \frac{(1 - \lambda \frac{b_0}{\omega})^2(\kappa'E' + \kappa E - \kappa\kappa') - m^2}{2}$$
$$+ \left(\frac{\lambda b_0}{2\omega} - \frac{b_0^2}{2\omega^2}\right) EE' + \frac{\lambda b_0 \omega - \boldsymbol{q}^2}{4}. \tag{18c}$$

Employing Eqs. (18) to get rid of the photon-polarization vectors in favor of the momenta in (16) we derive

$$\frac{1}{2}\sum_{s,s'}|\mathcal{M}|^2 \approx \frac{2Z^2e^6}{\omega^2(\boldsymbol{q}^2+\mu^2)^2}\mathrm{Re}\left\{\frac{(\boldsymbol{q}^2+\mu^2)(E^2+E'^2+4\frac{\lambda b_0}{\omega}EE')+4b_0^2 EE'}{(\kappa'+\frac{\lambda b_0}{2}+i\frac{E'}{\tau\omega})(\kappa-\frac{\lambda b_0}{2}-i\frac{E}{\tau\omega})} - 2\omega^2\left(\frac{\kappa'+\frac{\lambda b_0}{2}+i\frac{E'}{\tau\omega}}{\kappa-\frac{\lambda b_0}{2}-i\frac{E}{\tau\omega}} + \frac{\kappa-\frac{\lambda b_0}{2}-i\frac{E}{\tau\omega}}{\kappa'+\frac{\lambda b_0}{2}+i\frac{E'}{\tau\omega}}\right)\right.$$
$$\left. - 4\left[m^2 - \frac{\lambda b_0}{\omega}(EE' - m^2 + \omega^2)\right]\left(\frac{E'}{\kappa-\frac{\lambda b_0}{2}-i\frac{E}{\tau\omega}} - \frac{E}{\kappa'+\frac{\lambda b_0}{2}+i\frac{E'}{\tau\omega}}\right)^2 + \frac{\lambda 4 b_0}{\omega}\left(\frac{(E+E')E'}{\kappa-\frac{\lambda b_0}{2}+i\frac{E}{\tau\omega}} - \frac{(E+E')E}{\kappa'+\frac{\lambda b_0}{2}+i\frac{E'}{\tau\omega}}\right)\right\}. \tag{19}$$

The largest contributions come from the resonances at $2\omega\kappa - k^2 = 0$ and $2\omega\kappa' + k^2 = 0$. In the high-energy approximation these equations have a solution only for $m\omega - b_0 EE' \le 0$. This inequality can be equivalently expressed as the requirements $\omega \le \omega^*$ and $b_0\lambda > 0$ which is consistent with (14) and (15). Evidently, only one of the two photon polarizations (the one with $b_0\lambda > 0$) is resonant. As such, the differing polarization cases must be treated separately. Consider, for example the pole at

$$k^2 = 2\omega\kappa = 2p \cdot k \approx \omega E\left(\frac{m^2}{E^2} + \frac{k^2}{\omega^2} + \theta^2\right), \tag{20}$$

where θ is the angle between $\boldsymbol{k}$ and $\boldsymbol{p}$. The denominator of the corresponding fermion propagator is

$$\frac{1}{2p \cdot k - k^2 + iE/\tau} = \frac{1}{\omega E(\frac{m^2}{E\omega}\frac{\omega-\omega^*}{E-\omega^*} + \theta^2 + \frac{i}{\omega\tau})}, \tag{21}$$

where we used (15) to eliminate λb_0 in favor of ω^*,

$$k^2 \approx -\lambda b_0\omega = -\frac{\omega\omega^* m^2}{E(E-\omega^*)}, \qquad (\lambda b_0 > 0). \tag{22}$$

Note that (22) makes sense only when $\lambda b_0 > 0$, for otherwise ω^* is negative, indicating that there is no instability when $\lambda b_0 < 0$. Equation (21) implies that above the threshold, viz. when $\omega > \omega^*$, photon is radiated mostly at angles $\theta \lesssim \theta_0 = \sqrt{\frac{m^2}{E\omega}\frac{\omega-\omega^*}{E-\omega^*}}$. However, at and below the threshold, the angular distribution diverges at $\theta = \sqrt{\frac{m^2}{E\omega}\frac{\omega^*-\omega}{E-\omega^*}}$ which is regulated by the cutoff introduced in the previous section.

Let us now examine the photon propagator in the resonant case $\lambda b_0 > 0$. Writing $\boldsymbol{q}^2 = [(\boldsymbol{k} \times \boldsymbol{q})^2 + (\boldsymbol{k} \cdot \boldsymbol{q})^2]/\boldsymbol{k}^2$ and expanding at small-photon emission angles we obtain

$$\boldsymbol{q}^2 = -(k + p' - p)^2 \approx \theta^2 E^2 + \theta'^2 E'^2 - 2EE'\theta\theta'\cos\phi$$
$$+ \frac{1}{4}\left[\frac{m^2(\omega - \omega^*)}{E'(E - \omega^*)} - E\theta^2 + E'\theta'^2\right]^2. \tag{23}$$

In the nonanomalous case $\omega^* = 0$, and the momentum transfer is bounded from below by $\frac{m^4\omega^2}{4E^2E'^2}$. In contrast, in the presence of the anomaly the momentum transfer is allowed to vanish. We can find the corresponding kinematic region by first observing that the sum of the first three terms and the last term in the right-hand side of (23) are non-negative and therefore have to vanish independently. The sum of the first three terms vanishes only when $\phi = 0$ and $E\theta = E'\theta'$ in which case the momentum transfer reads

$$\boldsymbol{q}^2|_{\phi=0,E\theta=E'\theta'} \approx \frac{1}{4}\left[\frac{m^2(\omega - \omega^*)}{E'(E - \omega^*)} + \frac{\omega E}{E'}\theta^2\right]^2$$
$$= \frac{1}{4}\frac{\omega^2 E^2}{E'^2}\left[\frac{m^2(\omega - \omega^*)}{\omega E(E - \omega^*)} + \theta^2\right]^2. \tag{24}$$

This imbues the photon propagator with the same resonant behavior as the fermion propagator, as can be seen by comparing with (21). Apparently, we need to regulate the divergence at $\boldsymbol{q}^2 = 0$ by replacing $\theta^2 \to \theta^2 + \frac{i}{\omega\tau}$ in (24). This is tantamount to the replacement $\boldsymbol{q}^2 \to \boldsymbol{q}^2 + \frac{E^2}{4E'^2\tau^2}$. Along with the Debye mass μ introduced in (12) it provides the regulator of the photon propagator at small-momentum transfers,

$$q^2 \to q^2 + \frac{E^2}{4E'^2\tau^2} + \mu^2. \qquad (25)$$

The physics of bremsstrahlung in chiral medium is most transparent in two limiting cases: (i) low temperature $m \gg \mu$; and (ii) high temperature $\mu \gg m$. In the anomaly-free medium $b_0 = 0$, the first case reduces to the scattering off a single nucleus. In this case the momentum transfer $\boldsymbol{q}^2$ never vanishes. On the contrary, in the presence of anomaly, negative k^2 can drive the momentum transfer towards zero for one of the photon polarizations, as we explained.

A. Low temperature: $\mu \ll m$

We first consider the low-temperature/heavy-fermion regime. We also assume, for the sake of simplicity, that $\mu^2 \ll 1/\tau^2$ so that τ regulates both the fermion and the photon propagators. In the anomaly-free medium, the typical momentum transfer is of the order m and therefore the scattering cross section is insensitive to the cutoffs τ and μ. This conclusion is upended in the anomalous medium due to the resonances discussed in Sec. III.

The bremsstrahlung cross section is obtained by substituting (19) into (1) and integrating over the fermion and photon directions. The angular integrals are performed in Appendix B. The results are essentially different for positive and negative values of the parameter $b_0\lambda$. For $b_0\lambda < 0$ there are no resonances and the angular integrals simplify greatly. In this case, τ^{-1} and μ may be neglected given that all integrals are convergent. In this case the cross section reads,

$$\frac{d\sigma(b_0\lambda < 0)}{d\omega} \approx \frac{Z^2 e^6 E'}{4(2\pi)^3 (m^2\omega - \lambda b_0 EE')E} \left(\frac{E}{E'} + \frac{E'}{E} - \frac{2}{3}\right)$$
$$\times \left[\ln \frac{4E^2 E'^2}{\omega(m^2\omega - \lambda b_0 EE')} - 1\right]. \qquad (26)$$

In the anomaly-free medium $b_0 = 0$ (26) reduces to the well-known Bethe-Heitler expression for the bremsstrahlung cross section on a heavy nucleus [19,40],

$$\frac{d\sigma_{\rm BH}}{d\omega} \approx \frac{Z^2 e^6 E'}{4(2\pi)^3 m^2 \omega E} \left(\frac{E}{E'} + \frac{E'}{E} - \frac{2}{3}\right) \left(\ln \frac{2EE'}{m\omega} - \frac{1}{2}\right). \qquad (27)$$

The effect of the anomaly on this photon polarization is most significant in the infrared region $\omega \ll b_0 EE'/m^2$ where the cross section scales as $\log(1/\omega)$. In contrast, without the anomaly it scales as $(1/\omega)\log(1/\omega)$. Thus, the anomaly tends to suppress emission of photons with $b_0\lambda < 0$ polarization.

The situation is essentially different for the $b_0\lambda > 0$ polariziation since the corresponding cross section diverges in the limit $\tau^{-1} \to 0$, i.e., at small photon emission angles when $\omega \le \omega^*$. As we explained in the previous section, this divergence occurs concurrently in the fermion and the photon propagators and is regulated by shifting $\theta^2 \to \theta^2 + \frac{i}{\omega\tau}$ and similarly for θ'. Keeping only the essential terms and setting $\mu = 0$ we obtain,

$$\frac{d\sigma(b_0\lambda > 0)}{d\omega} \approx \frac{Z^2 e^6 E'}{4(2\pi)^3 Em^2\omega} \left\{ \frac{\left(\frac{E}{E'} + \frac{E'}{E} - \frac{2}{3}\right)\left(\ln \frac{4E^2 E'^2}{m^2\omega^2 \sqrt{\frac{E^2(\omega^*-\omega)^2}{\omega^2(E-\omega^*)^2} + \frac{4E^4 E'^2}{m^4\omega^4\tau^2}}} - 1\right)}{\sqrt{\frac{E^2(\omega^*-\omega)^2}{\omega^2(E-\omega^*)^2} + \frac{4E^4}{m^4\omega^2\tau^2}}} + \frac{2m^4(\omega^*-\omega)\tau^3}{E^3 E'^4 (E-\omega^*)} \left[E'^6 \arctan \frac{m^2(\omega^*-\omega)\tau}{E'(E-\omega^*)} \right. \right.$$

$$\left. \left. + E^6 \arctan \frac{m^2(\omega^*-\omega)\tau}{E(E-\omega^*)} \right] \Theta(\omega^*-\omega) \right\}, \qquad (28)$$

where Θ is the step function and we replaced $b_0\lambda$ in favor of ω^* using (22).

The are two kinds of terms in (28): (i) The first line of (28) reduces to the anomaly-free result (27) in the limit $b_0 \to 0$ and $E/\tau \to 0$. We neglected all terms proportional to τ^{-1} with exception of those appearing under the radicals where their role is to regulate the divergence at the threshold $\omega = \omega^*$; (ii) The second and the third lines of (28) represent the most singular resonance contributions, viz. the terms that are most divergent at small τ^{-1}. In the limit $b_0 \to 0$ the step function can only be satisfied when $\omega \to 0$, hence the anomalous contribution vanishes.

We stress that the chiral resonance in the fermion propagator contributes only to one of the photon polarizations, namely $b_0\lambda > 0$. The other polarization $b_0\lambda < 0$ is suppressed. This is in contrast to the lack of a distinction between handedness in the absence of the anomaly. A remarkable feature of the anomalous contribution, dominated by the second and the third lines of (28), is that at small ω its spectrum scales as $1/\omega$, which is the same form as the soft-photon spectrum without the chiral anomaly (27).

The bremsstrahlung photon spectra are plotted in Fig. 2. Inspection of Fig. 2 reveals two significant features. Firstly, at $\omega < \omega^*$ the cross section is enhanced as

compared to the Bethe-Heitler formula. To better understand the parametric dependence of the cross section, consider the soft photon region $\omega \ll \omega^* \ll E$, in particular $\omega^* \approx \lambda b_0 E^2/m^2$. Equation (28) can be written as

$$\frac{d\sigma(b_0\lambda > 0)}{d\omega} \approx \frac{3\pi}{2} \frac{m^2\tau^3 b_0}{\ln\frac{2E^2}{m\omega}} \frac{d\sigma_{\rm BH}}{d\omega}. \tag{29}$$

Since $m\tau \gg b_0\tau \gg 1$ we indeed observe that the anomalous cross section is strongly enhanced in the soft-photon region. Secondly, when focusing on the production of the right-handed photons, we see a sharp cutoff at $\omega = \omega^*$. The anomalous contribution vanishes at higher-photon energies. A similar behavior was discussed in our paper [15] for the case of magnetic moment contribution.

To complete our discussion, we cite here the magnetic moment contribution to the bremsstrahlung in the semi-soft photon limit $b_0 \ll \omega \ll E$ computed in [15]:

$$\frac{d\sigma_M}{d\omega} \approx \frac{2e^4\mathbb{M}^2}{3(2\pi)^3\omega}\left[\frac{3b_0^2}{m^2}\ln\left(\frac{4E^4}{m^2\omega^2}\right) + \ln^2\frac{4E^2}{m^2}\right.$$
$$\left. + \frac{2b_0^4\pi}{m^2\Gamma^2}\Theta(\omega_0 - \omega)\right], \tag{30}$$

where $\mathbb{M}$ is the magnetic moment. In Fig. 2 one can see that it gives a minor correction to the total cross section, even though it exhibits qualitative features similar to (26) and (28). Overall the anomaly in the magnetic channel may amplify photon production over a wider range of frequencies but produces less radiation when compared to the electric channel.

B. High temperatures: $\mu \gg m$

We now consider the differential cross section in the opposite limit where $\mu \gg m$ and $\mu^2 \gg 1/\tau^2$, so that τ^{-1} is neglected in the photon propagator. We assume that the projectile fermion experiences only a single hard scattering and therefore its propagator is the same as in a vacuum [22,23]. The process of computing the differential cross section and the necessary integrals is similar to the one outlined in Appendix B, except that m may be taken to zero in the high-temperature limit. It is well-known that μ not only regulates the Coulomb pole, but also sets the smallest photon emission angle $\theta_{\min} = \mu/E \ll 1$ [23,41]. In the previous subsection both roles were played by m. In the high-energy limit, one can take the integrals $I_{j,n,l}$, by expanding the integrands at small-photon emission angles θ and θ',

$$I_{j,n,l} \approx \int \frac{d\Omega' d\Omega_k}{[(E^2\theta^2 - 2EE'\theta\theta'\cos\phi + E'^2\theta'^2) + \frac{1}{4}(E\theta^2 - E'\theta'^2 + \lambda b_0)^2]^j}$$
$$\times \frac{1}{[(E\omega\theta^2 - \lambda b_0 E')^n - (-i\frac{E}{\tau})^n][(E'\omega\theta'^2 - \lambda b_0 E)^l - (i\frac{E'}{\tau})^l]}, \tag{31}$$

where ϕ is the azimuthal angle which may be integrated over directly. As an example consider $I_{1,1,1}$. Integrating of ϕ yields,

$$I_{1,1,1} \approx \int_{\frac{\mu^2}{E^2}}^{\infty} \int_{\frac{\mu^2}{E'^2}}^{\infty} \frac{\pi^2 d\theta'^2 d\theta^2}{\sqrt{((E^2\theta^2 + E'^2\theta'^2) + \frac{1}{4}(E\theta^2 - E'\theta'^2 + \lambda b_0)^2)^2 - 4E^2E'^2\theta^2\theta'^2}}$$
$$\times \frac{1}{((E\omega\theta^2 - \lambda b_0 E') + i\frac{E}{\tau})((E'\omega\theta'^2 - \lambda b_0 E) - i\frac{E'}{\tau})}, \tag{32}$$

where we replaced the upper integration limits by infinities thanks to the fast convergence of the integrals. Taking the remaining integrals we find that $I_{1,1,1}$ gives the following contribution to the differential cross section:

$$I_{1,1,1} \approx \frac{4\pi^2 \ln\frac{4E^2E'^2}{\sqrt{(\mu^2\omega^2 - \lambda b_0\omega EE')^2 + 4\frac{E^4E'^2}{\tau^2}}}}{\omega EE'\sqrt{(\mu^2\omega - \lambda b_0 EE')^2 + 4\frac{E^3E'}{\tau^2}}}. \tag{33}$$

The other terms may be computed in a similar fashion. In those integrals where the integral over θ (or θ') is not convergent at large angles, one needs to first integrate over the region $\theta < \theta'$ (or $\theta' < \theta$); the remaining integral then converges well. The result of the calculation is different for the two photon polarziations and reads

$$\frac{d\sigma(b_0\lambda < 0)}{d\omega} \approx \frac{Z^2 e^6 E'}{4(2\pi)^3(\mu^2\omega - \lambda b_0 EE')E}\left(\frac{E}{E'} + \frac{E'}{E}\right)\left[\ln\frac{4E^2E'^2}{\mu^2\omega^2 - \lambda b_0\omega EE'} - 1\right], \tag{34}$$

$$\frac{d\sigma(b_0\lambda > 0)}{d\omega} \approx \frac{Z^2 E' e^6}{4(2\pi)^3 E\mu^2\omega} \left\{ \frac{\mu^2\omega(\frac{E}{E'} + \frac{E'}{E})[\ln\frac{4E^2E'^2}{\sqrt{(\mu^2\omega^2 - \lambda b_0\omega EE')^2 + 4\frac{E^4 E'^2}{\tau^2}}} - 1]}{\sqrt{(\mu^2\omega - \lambda b_0 EE')^2 + \frac{E^3 E'}{\tau^2}}} \right.$$

$$\left. + \frac{\lambda b_0 \mu\tau}{E}\arctan\left(\frac{(\lambda b_0 EE' - \mu^2\omega)\tau}{EE'}\right)\Theta(\omega^* - \omega) \right\}, \tag{35}$$

where ω^* is given by (15) and $E', E \gg \mu$.

Consider the soft-photon limit in a medium such that $\mu \gg m \gg \tau^{-1}$. The soft-photons region corresponds to $\omega \ll E$ and $\omega \ll \omega^*$, the latter condition implying $\omega \ll b_0 E^2/m^2$. Then (35) reduces to

$$\frac{d\sigma(b_0\lambda > 0)}{d\omega} \approx \frac{\pi}{2}\frac{\mu}{E}\frac{b_0\tau}{\ln\frac{2E^2}{\mu\omega}}\frac{d\sigma_{\text{BH}}}{d\omega}, \tag{36}$$

where the Bethe-Heitler cross section in this case is obtained by setting $b_0 = 0$ in (34). One observes only a modest enhancement, if any, as compared to (29).

V. ENERGY LOSS

A fast particle moving across a medium loses energy. There are two main mechanisms for energy loss at sufficiently high energies. The collisional energy loss occurs due to momentum transfer in the course of elastic collisions. The radiative energy loss is caused by the bremsstrahlung. Comprehensive discussions of the energy-loss regimes and phenomenological applications can be found in [42,43]. In chiral media there are additional contributions to the energy loss driven by the chiral anomaly. The results of the previous section allow us to compute the amount of energy lost due to the bremsstrahlung in a scattering off a single source of electric charge eZ.

Throughout this paper we neglected the quantum interference effects assuming that the photon formation time t_f is much shorter than the mean-free-path ℓ. In this approximation the energy loss per unit length is

$$-\frac{dE}{dz} = n\int_0^E \omega\frac{d\sigma^{eZ\to eZ\gamma}}{d\omega}d\omega, \tag{37}$$

where n is number of scatterers per unit volume which can be expressed in terms of the elastic scattering cross section $n = 1/\ell\sigma^{eZ\to eZ}$. At high energies,

$$\sigma^{eZ\to eZ} = \frac{\alpha(eZ)^2}{\max\{\mu^2, m^2\}} + \mathcal{O}(\mathbb{M}), \tag{38}$$

where $\alpha = e^2/4\pi$. The omitted term in (38) is proportional to the small magnetic moment $\mathbb{M}$ of the source. Actually, this term is affected by the anomaly and can become

essential at very high energies [44]. However, in the present calculation it can be neglected.

As in the previous section we will be concerned with the two limits.

A. Low temperatures: $\mu \ll m$

Substituting (26) or (28) into (37) and integrating over ω gives the energy loss for two photon polarizations. For brevity we will record these expressions in the limit $m^2 \gg b_0 E$,

$$-\frac{dE(b_0\lambda < 0)}{dz} \approx \frac{e^2 E}{16\pi^2\ell}\left[\ln\frac{2E}{m} - \frac{1}{3} - \frac{2b_0 E}{9m^2}\left(\pi + 2\ln\frac{E}{b_0}\right)\right], \tag{39}$$

$$-\frac{dE(b_0\lambda > 0)}{dz} \approx \frac{e^2 E}{16\pi^2\ell}\left\{\ln\frac{2E}{m} - \frac{1}{3} + \frac{2b_0 E}{9m^2}\left(\pi + 2\ln\frac{E}{b_0}\right)\right.$$
$$\left. + 2\tau(E - \omega^*)\arctan\frac{2m^2\omega^*\tau}{E(E - \omega^*)}\right\}. \tag{40}$$

Equation (39) agrees with Eq. (93.24) in [40] when $b_0 = 0$. We observe that the anomaly slightly reduces the amount of energy lost due to the bremsstrahlung of $b_0\lambda < 0$ photons. This is consistent with our discussion in the previous section that the bremsstrahlung cross section is reduced in this case.

As far as the $b_0\lambda > 0$ polarization is concerned, we consider again the soft photon region $\omega \ll \omega^* \ll E$ were $\lambda b_0 \ll m$ so that the last term on the right-hand side of (40) is dominant. This allows us to cast the energy loss (40) in a convenient form,

$$-\frac{dE(b_0\lambda > 0)}{dz} \approx \frac{\pi\tau E}{\ln\frac{2E}{m}}\left(-\frac{dE}{dz}\right)_{\text{BH}}. \tag{41}$$

Thus, the energy loss due to the chiral anomaly is driven by the $b_0\lambda > 0$ photon polarization and is enhanced by the large factor τE over the Bethe-Heitler result.

B. High temperature: $\mu \gg m$

The rate of energy loss in the high-temperature limit is computed similarly. Plugging (35) and (37) into (37) we derive

$$-\frac{dE(b_0\lambda<0)}{dz}\approx\frac{e^2E}{16\pi^2\ell}\left(\ln\frac{2E}{\mu}-\frac{6b_0E}{7\mu^2}\ln\frac{E}{b_0}\ln\frac{4E^2}{\mu^2}\right),\quad(42)$$

$$-\frac{dE(b_0\lambda>0)}{dz}\approx\frac{e^2E}{16\pi^2\ell}\left(\ln\frac{2E}{\mu}+\frac{6b_0E}{7\mu^2}\ln\frac{E}{b_0}\ln\frac{4E^2}{\mu^2}+\frac{2b_0\mu\tau}{3E}\right).$$
$$(43)$$

Equation (42) agrees with [41] when $b_0=0$. As in the low-temperature case, the energy loss is mostly driven by $b_0\lambda>0$ polarization. However, the overall magnitude of the lost energy sensitively depends on the actual values of the parameters.

The total energy loss is given by the sum of (39) and (39) (when $\mu\ll m$) and of (42) and (43) (when $\mu\gg m$). We observe that the chirality dependent nonresonant contributions cancel out, while the resonant terms proportional to τ remain. Thus the total energy loss is also chirality dependent which may facilitate its experimental observation.

VI. SUMMARY

In this paper we computed and analyzed the spectrum of electromagnetic radiation emitted by a fast particle traveling in the chiral medium supporting the chiral magnetic current with constant chiral conductivity b_0. We observed in Fig. 2 that at low temperatures $\mu\ll m$ the anomalous contribution to bremsstrahlung, stemming from one of the photon polarizations, is several orders of magnitude larger than the nonanomalous one. We also computed the corresponding enhancement of the energy loss. If confirmed by experimental observation, it can serve as an effective tool to study the chiral anomaly in the materials. It can also be used to search for the new forms of the chiral matter. In particular, a cosmic ray moving through the chiral domain generated by an axion field would radiate and lose energy in a peculiar way described in this paper. In the opposite

limit of very high temperatures, $\mu\gg m$, the effect of the anomaly is much smaller as seen in Fig. 3.

In arriving at our conclusions we made a number of assumptions. First of all, we treated the chiral conductivity b_0 as a constant. However, it does evolve in time albeit slowly. Its temporal evolution is characterized by the relaxation time τ, which we assumed to be the large parameter in our calculation. The spatial extent of the domain can be neglected as long as it is larger than photon formation time t_f which is a very good approximation considering that the formation time must be shorter than the mean free path ℓ in the Bethe-Heitler limit. Also, for the sake of simplicity we neglected the chiral displacement $\boldsymbol{b}$. The electric current $\boldsymbol{j}=\boldsymbol{b}\times\boldsymbol{\mathcal{E}}$ is induced at finite $\boldsymbol{b}$ and is responsible for the anomalous Hall effect. At $b_0=0$ it induces the radiative instability of the chiral matter which is similar in many ways to the homogeneous and isotropic case $b_0\neq0$, $\boldsymbol{b}=0$, especially at high energies [45,46]. In fact, one can obtain the rate of the Cherenkov radiation by simply replacing $b_0\to|\boldsymbol{b}|\cos\beta$, where β is the angle between $\boldsymbol{b}$ and $\boldsymbol{k}$. The relationship between the two cases is more delicate for bremmstrahlung. The photon propagator takes now the following form, in place of (5):

$$D_{00}=\frac{i\boldsymbol{q}^2}{\boldsymbol{q}^4+(\boldsymbol{b}\times\boldsymbol{q})^2},\tag{44}$$

$$D_{0i}=\frac{(\boldsymbol{b}\times\boldsymbol{q})_i}{\boldsymbol{q}^4+(\boldsymbol{b}\times\boldsymbol{q})^2},\tag{45}$$

$$D_{ij}=-\frac{i}{\boldsymbol{q}^4+(\boldsymbol{b}\times\boldsymbol{q})^2}\left\{\boldsymbol{q}^2\delta_{ij}+b_ib_j-\frac{[\boldsymbol{q}^4-(\boldsymbol{b}\cdot\boldsymbol{q})^2]q_iq_j}{\boldsymbol{q}^4}\right.$$
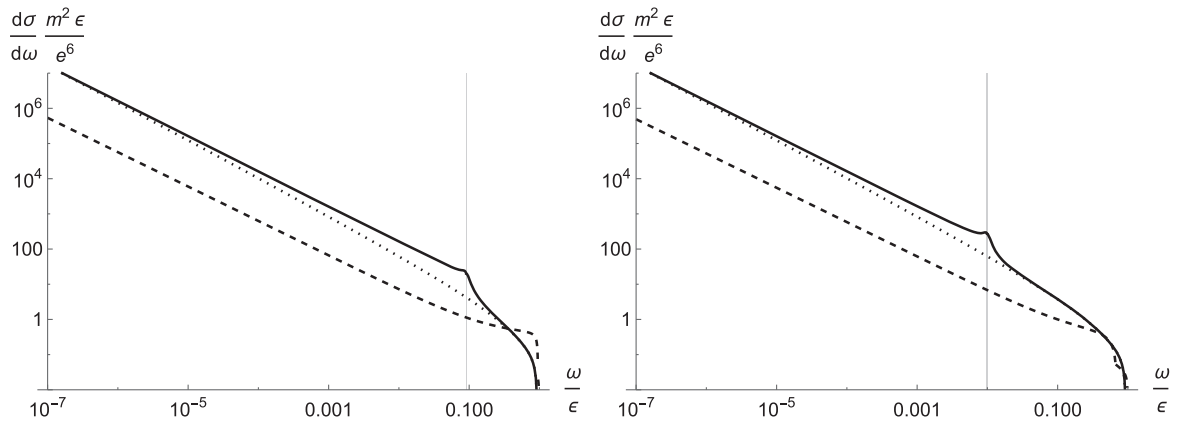$$\left.-\frac{\boldsymbol{b}\cdot\boldsymbol{q}}{\boldsymbol{q}^2}(b_iq_j+b_jq_i)\right\}.\tag{46}$$

FIG. 3.   The bremsstrahlung spectrum at $\mu\gg m$. The solid line is the high-energy approximation given by the sum of Eqs. (34) and (35), the dotted line is the Bethe-Heitler limit $b_0=0$, and the dashed line is the magnetic moment contribution (30). Left panel: $b_0=10^{-1}m$, right panel: $b_0=10^{-2}m$, both panels: $E=10^2m$, $\mu=10m$, $\tau^{-1}=\Gamma=0.1b_0$, $Z=33$. The vertical line indicates ω^*/E.

The denominator of the D_{00} component that drives the electric channel is merely shifted $\mu^2 \to \mu^2 + (\boldsymbol{b} \times \hat{\boldsymbol{q}})^2$. The corresponding energy loss is anisotropic as it depends on the angle between the incident fermion momentum and the displacement vector. Otherwise, we believe that the qualitative similarity will persist. The magnetic channel is quite different, but its contribution to the overall energy loss is not significant. Clearly, due to possible applications to Weyl and Dirac semi-metals, the case of finite $\boldsymbol{b}$ deserves a dedicated study.

Another critical assumption we made is that photon formation time t_f is much shorter than the mean-free path ℓ. As argued in [41], the condition $t_f \ll \ell$ translates into the requirement that $m, \mu \ll E \ll \mu\sqrt{\omega\ell}$. Since t_f is proportional to ω, this approximation breaks down at high energies where one must take account of the multiple scatterings of the projectile in the medium. The resulting Landau-Pomeranchuk-Migdal quantum interference effect [47,48] is an important feature of the bremsstrahlung spectrum and must certainly be taken into account at higher energies.

Throughout this paper, we have treated the chiral anomaly as it pertains to QED. The non-Abelian version of the chiral anomaly has a similar effect in QCD generating contributions to gluon and photon bremsstrahlung. Calculation of bremsstrahlung and energy loss in QCD in the presence of the chiral magnetic current is relevant to the quark-gluon plasma phenomenology. We plan to address this elsewhere.

ACKNOWLEDGMENTS

APPENDIX A: THE BREMSSTRAHLUNG CROSS SECTION AT THE LEADING ORDER

The bremsstrahlung cross section corresponding to Fig. 1 including the cutoffs reads,

$$
\begin{aligned}
d\sigma = \sum_\lambda \frac{Z^2 \omega e^6 d\omega}{16(2\pi)^5} \frac{|\boldsymbol{p}'|}{|\boldsymbol{p}|} \mathrm{Re} \Bigg\{ & (2E^2 + 2E'^2 + k^2)I_{1,1,1} - \frac{\omega^2 + \boldsymbol{k}^2}{4k^2}(I_{2,1,-1} + I_{2,-1,1}) + (I_{1,0,1} - I_{1,1,0}) \\
& + \frac{2m^2(\omega^2 + \boldsymbol{k}^2) + 4EE'k^2 + k^4}{4k^2}(I_{1,2,0} - 2I_{1,1,1} + I_{1,0,2}) - \frac{4}{k^2}\Big[m^2\boldsymbol{k}^2(E'^2 I_{2,2,0} - 2EE'I_{2,1,1} + E^2 I_{2,0,2}) \\
& + \frac{\boldsymbol{k}^2 k^2}{2}(E^2 I_{2,0,2} + E'^2 I_{2,2,0}) + E'^2 E'^2 k^2(I_{2,2,0} - 2I_{2,1,1} + I_{2,0,2}) - EE'k^2(I_{2,0,1} + I_{2,1,0}) \Big] \\
& + 4\pi^2 \frac{\mathrm{arctanh}\left(\frac{2|\boldsymbol{k}||\boldsymbol{p}|}{2\omega E - k^2 + i\frac{E}{\tau}}\right)\mathrm{arctanh}\left(\frac{2|\boldsymbol{k}||\boldsymbol{p}'|}{2\omega E' + k^2 - i\frac{E'}{\tau}}\right)}{k^2 |\boldsymbol{p}||\boldsymbol{p}'|} - k^2(4\pi)^2 \frac{\mathrm{arctanh}\left(\frac{2\omega E + 2|\boldsymbol{p}||\boldsymbol{k}| - k^2 + \mu^2}{\mu|\boldsymbol{p}'|}\right) - \mathrm{arctanh}\left(\frac{2\omega E + 2|\boldsymbol{p}||\boldsymbol{k}| - k^2 + \mu^2}{\mu|\boldsymbol{p}'|}\right)}{k^3 |\boldsymbol{p}||\boldsymbol{p}'|\mu} \Bigg\},
\end{aligned}
\tag{A1}
$$

where the angular integrals $I_{j,n,l}$ are defined as

$$
I_{j,n,l} = \int \frac{d\Omega' d\Omega_k}{(\boldsymbol{q}^2 + \mu^2)^j[(2\omega\kappa - k^2)^n - (-i\frac{E}{\tau})^n][(2\omega\kappa' + k^2)^l - (i\frac{E'}{\tau})^l]},
\tag{A2}
$$

where j, n, l are integers, $k^2 = -\lambda b_0|\boldsymbol{k}|$. When any of these integers is negative the corresponding cutoffs can be set to zero.

APPENDIX B: INTEGRALS $I_{j,n,l}$ IN THE ULTRARELATIVISTIC HEAVY FERMION LIMIT

An analysis of (19) reveals several dominant contributions to the differential ultrarelativistic cross section in terms of $I_{j,n,l}$. We consider these contributions under two different regimes. In the first, we consider the case of heavy fermions relative to the Debye mass such that $\mu \ll m$, $\mu^2 \ll E/\tau$, and in the second we consider the case of high temperature which takes on the opposite limit $m \ll \mu$. We focus on the first case in this appendix, however in both cases we take the high-energy limit $\mu, m \ll E, E'$ and $\omega \gg b_0$. Additionally, the dominance of small emission angles allows us to neglect the contribution due to large angles. Letting θ and θ' be the angles between $\boldsymbol{k}$ and $\boldsymbol{p}$, and $\boldsymbol{k}$ and $\boldsymbol{p}'$ leads to the following approximation:

$$I_{j,n,l} \approx \int \frac{d\Omega' d\Omega_k}{\left[\left(E^2\theta^2 - 2E'E\theta\theta'\cos\phi + E'^2\theta'^2\right) + \frac{1}{4}\left(\frac{m^2\omega}{EE'} - E\theta^2 + E'\theta'^2 - \lambda b_0 + \frac{2i}{\omega\tau}\right)^2\right]^j}$$

$$\times \frac{1}{\left[\left(E\omega\theta^2 + \frac{m^2\omega - \lambda b_0 E'E}{E}\right)^n - \left(-i\frac{2E}{\tau}\right)^n\right]\left[\left(E'\omega\theta'^2 + \frac{m^2\omega - \lambda b_0 E'E}{E'}\right)^l - \left(i\frac{2E'}{\tau}\right)^l\right]}, \tag{B1}$$

where ϕ is the azimuthal angle ranging from 0 to 2π. Integrating up to emission angles for the two possible cases $j = 1, 2$

$$I_{1,n,l} \approx \int \frac{\pi^2 d\theta'^2 d\theta^2}{\sqrt{\left[E^2\theta^2 + E'^2\theta'^2 + \frac{1}{4}\left(\frac{m^2\omega}{EE'} - E\theta^2 + E'\theta'^2 - \lambda b_0 + \frac{2i}{\omega\tau}\right)^2\right]^2 - 4E'^2 E^2 \theta^2 \theta'^2}}$$

$$\times \frac{1}{\left[\left(E\omega\theta^2 + \frac{m^2\omega - \lambda b_0 E'E}{E}\right)^n - \left(-i\frac{2E}{\tau}\right)^n\right]\left[\left(E'\omega\theta'^2 + \frac{m^2\omega - \lambda b_0 E'E}{E'}\right)^l - \left(i\frac{2E'}{\tau}\right)^l\right]}, \tag{B2}$$

$$I_{2,n,l} \approx \int \frac{\left[E^2\theta^2 + E'^2\theta'^2 + \frac{1}{4}\left(\frac{m^2\omega}{EE'} - E\theta^2 + E'\theta'^2 - \lambda b_0\right)^2 + \mu^2\right]\pi^2 d\theta'^2 d\theta^2}{\left\{\left[E^2\theta^2 + E'^2\theta'^2 + \frac{1}{4}\left(\frac{m^2\omega}{EE'} - E\theta^2 + E'\theta'^2 - \lambda b_0 + \frac{2i}{\omega\tau}\right)^2\right]^2 - 4E'^2 E^2 \theta^2 \theta'^2\right\}^{\frac{3}{2}}}$$

$$\times \frac{1}{\left[\left(E\omega\theta^2 + \frac{m^2\omega - \lambda b_0 E'E}{E}\right)^n - \left(-i\frac{2E}{\tau}\right)^n\right]\left[\left(E'\omega\theta'^2 + \frac{m^2\omega - \lambda b_0 E'E}{E'}\right)^l - \left(i\frac{2E'}{\tau}\right)^l\right]}. \tag{B3}$$

These integrals may then be taken for the relevant factors of n and l, noting the dominance of the regions $\omega E^2\theta^2 < \sqrt{(m^2\omega - \lambda b_0 E'E)^2 + \frac{E^4}{\tau^2}}$ and $\omega E'^2\theta'^2 < \sqrt{(m^2\omega - \lambda b_0 E'E)^2 + \frac{E'^4}{\tau^2}}$, acting as effective bounds for the integration. It is convenient to replace the integrals over emission angles with the difference $\Delta = |E\theta - E'\theta'|$ given that the integrands are largest at $\Delta = 0$. The results for various relevant integrals for the differential cross section are given. For instances

$$I_{1,1,1} \approx \frac{4\pi^2 \ln\frac{4E^2 E'^2}{\sqrt{(m^2\omega^2 - \lambda b_0 \omega EE')^2 + \frac{16E^4 E'^2}{\tau^2}}}}{\omega EE' \sqrt{(m^2\omega - \lambda b_0 EE')^2 + \frac{16E^3 E'}{\tau}}} \tag{B4}$$

and

$$I_{1,-1,1} + I_{1,1,-1} \approx \frac{4\pi^2}{\omega\sqrt{(m^2\omega - \lambda b_0 EE')^2 + \frac{16E^3 E'}{\tau^2}}}\left(\frac{E'}{E} + \frac{E}{E'}\right). \tag{B5}$$

Other integrals are more easily taken together, such as

$$E'^2 I_{2,2,0} - 2EE' I_{2,1,1} + E^2 I_{2,0,2} \approx \frac{8\pi^2 \ln\frac{4E^2 E'^2}{\sqrt{(m^2\omega^2 - \lambda b_0 \omega EE')^2 + \frac{16E^4 E'^2}{\tau^2}}}}{3[(m^2\omega - \lambda b_0 EE')^2 + \frac{16E^3 E'}{\tau^2}]} \frac{\pi^2\tau^3}{4E^4 E'^4 \omega}\left[E'^6 \arctan\frac{m^2(\omega^* - \omega)\tau}{E'(E - \omega^*)}\right.$$

$$\left. + E^6 \arctan\frac{m^2(\omega^* - \omega)\tau}{2E(E - \omega^*)}\right]\Theta(\omega^* - \omega), \tag{B6}$$

where ω^* is given by (15). The remaining integrals may be computed similarly, or related using the symmetry $p \to -p'$ such that

$$2\omega\kappa - k^2 \to -(2\omega\kappa' + k^2), \qquad \boldsymbol{q}^2 = -(p' - p + k)^2 \to -(-p + p' + k)^2 = \boldsymbol{q}^2. \tag{B7}$$

[1] S. L. Adler, Axial vector vertex in spinor electrodynamics, Phys. Rev. **177,** 2426 (1969).

[2] J. S. Bell and R. Jackiw, A PCAC puzzle: $\pi^0 \to \gamma\gamma$ in the σ model, Nuovo Cimento A **60,** 47 (1969).

[3] D. Kharzeev, Parity violation in hot QCD: Why it can happen, and how to look for it, Phys. Lett. B **633,** 260 (2006).

[4] D. Kharzeev and A. Zhitnitsky, Charge separation induced by P-odd bubbles in QCD matter, Nucl. Phys. **A797,** 67 (2007).

[5] K. Fukushima, D. E. Kharzeev, and H. J. Warringa, The chiral magnetic effect, Phys. Rev. D **78,** 074033 (2008).

[6] D. E. Kharzeev, Topologically induced local P and *CP* violation in QCD x QED, Ann. Phys. (Amsterdam) **325,** 205 (2010).

[7] D. E. Kharzeev, L. D. McLerran, and H. J. Warringa, The effects of topological charge change in heavy ion collisions: 'Event by event P and *CP* violation', Nucl. Phys. **A803,** 227 (2008).

[8] F. R. Klinkhamer and G. E. Volovik, Emergent *CPT* violation from the splitting of Fermi points, Int. J. Mod. Phys. A **20,** 2795 (2005).

[9] Q. Li, D. E. Kharzeev, C. Zhang, Y. Huang, I. Pletikosic, A. V. Fedorov, R. D. Zhong, J. A. Schneeloch, G. D. Gu, and T. Valla, Observation of the chiral magnetic effect in ZrTe5, Nat. Phys. **12,** 550 (2016).

[10] P. O. Sukhachov, V. A. Miransky, I. A. Shovkovy, and E. V. Gorbar, Collective excitations in Weyl semimetals in the hydrodynamic regime, J. Phys. Condens. Matter **30,** 275601 (2018).

[11] A. R. Zhitnitsky, P odd fluctuations and long range order in heavy ion collisions. Deformed QCD as a toy model, Nucl. Phys. **A897,** 93 (2013).

[12] D. E. Kharzeev, J. Liao, S. A. Voloshin, and G. Wang, Chiral magnetic and vortical effects in high-energy nuclear collisions—A status report, Prog. Part. Nucl. Phys. **88,** 1 (2016).

[13] P. Sikivie, Invisible axion search methods, Rev. Mod. Phys. **93,** 015004 (2021).

[14] J. Hansen and K. Tuchin, Collisional energy loss and the chiral magnetic effect, Phys. Rev. C **104,** 034903 (2021).

[15] J. Hansen and K. Tuchin, Bremsstrahlung in chiral medium: Anomalous magnetic contribution to the Bethe-Heitler formula, Phys. Rev. D **105,** 116008 (2022).

[16] S. M. Carroll, G. B. Field, and R. Jackiw, Limits on a Lorentz and parity violating modification of electrodynamics, Phys. Rev. D **41,** 1231 (1990).

[17] R. Lehnert and R. Potting, Vacuum Cerenkov radiation, Phys. Rev. Lett. **93,** 110402 (2004).

[18] K. Tuchin, Radiative instability of quantum electrodynamics in chiral matter, Phys. Lett. B **786,** 249 (2018).

[19] H. Bethe and W. Heitler, On the stopping of fast particles and on the creation of positive electrons, Proc. R. Soc. A **146,** 83 (1934).

[20] Z. Qiu, G. Cao, and X.-G. Huang, On electrodynamics of chiral matter, Phys. Rev. D **95,** 036002 (2017).

[21] M. Laine, O. Philipsen, P. Romatschke, and M. Tassler, Real-time static potential in hot QCD, J. High Energy Phys. 03 (2006) 054.

[22] X.-N. Wang, M. Gyulassy, and M. Plumer, The LPM effect in QCD and radiative energy loss in a quark gluon plasma, Phys. Rev. D **51,** 3436 (1995).

[23] R. Baier, Y. L. Dokshitzer, A. H. Mueller, S. Peigne, and D. Schiff, The Landau-Pomeranchuk-Migdal effect in QED, Nucl. Phys. **B478,** 577 (1996).

[24] M. Joyce and M. E. Shaposhnikov, Primordial magnetic fields, right-handed electrons, and the Abelian anomaly, Phys. Rev. Lett. **79,** 1193 (1997).

[25] A. Boyarsky, J. Frohlich, and O. Ruchayskiy, Self-consistent evolution of magnetic fields and chiral asymmetry in the early universe, Phys. Rev. Lett. **108,** 031301 (2012).

[26] D. E. Kharzeev, The chiral magnetic effect and anomaly-induced transport, Prog. Part. Nucl. Phys. **75,** 133 (2014).

[27] Z. V. Khaidukov, V. P. Kirilin, A. V. Sadofyev, and V. I. Zakharov, On magnetostatics of chiral media, Nucl. Phys. **B934,** 521 (2018).

[28] V. P. Kirilin, A. V. Sadofyev, and V. I. Zakharov, Anomaly and long-range forces, in *Pomeranchuk 100* (World Scientific, Singapore, 2014), pp. 272–286.

[29] Y. Akamatsu and N. Yamamoto, Chiral plasma instabilities, Phys. Rev. Lett. **111,** 052002 (2013).

[30] A. Avdoshkin, V. P. Kirilin, A. V. Sadofyev, and V. I. Zakharov, On consistency of hydrodynamic approximation for chiral media, Phys. Lett. B **755,** 1 (2016).

[31] M. Dvornikov and V. B. Semikoz, Magnetic field instability in a neutron star driven by the electroweak electron-nucleon interaction versus the chiral magnetic effect, Phys. Rev. D **91,** 061301 (2015).

[32] K. Tuchin, Electromagnetic field and the chiral magnetic effect in the quark-gluon plasma, Phys. Rev. C **91,** 064902 (2015).

[33] C. Manuel and J. M. Torres-Rincon, Dynamical evolution of the chiral magnetic effect: Applications to the quark-gluon plasma, Phys. Rev. D **92,** 074018 (2015).

[34] P. V. Buividovich and M. V. Ulybyshev, Numerical study of chiral plasma instability within the classical statistical field theory approach, Phys. Rev. D **94,** 025009 (2016).

[35] G. Sigl and N. Leite, Chiral magnetic effect in protoneutron stars and magnetic field spectral evolution, J. Cosmol. Astropart. Phys. 01 (2015) 025.

[36] X.-l. Xia, H. Qin, and Q. Wang, Approach to Chandrasekhar-Kendall-Woltjer state in a chiral plasma, Phys. Rev. D **94,** 054042 (2016).

[37] D. B. Kaplan, S. Reddy, and S. Sen, Energy conservation and the chiral magnetic effect, Phys. Rev. D **96,** 016008 (2017).

[38] V. P. Kirilin and A. V. Sadofyev, Anomalous transport and generalized axial charge, Phys. Rev. D **96,** 016019 (2017).

[39] M. Mace, N. Mueller, S. Schlichting, and S. Sharma, Chiral instabilities and the onset of chiral turbulence in QED plasmas, Phys. Rev. Lett. **124,** 191604 (2020).

[40] V. B. Berestetskii, E. M. Lifshitz, and L. P. Pitaevskii, *Quantum Electrodynamics*, Course of Theoretical Physics Vol. 4 (Pergamon Press, Oxford, 1982).

[41] R. Baier, Y. L. Dokshitzer, S. Peigne, and D. Schiff, Induced gluon radiation in a QCD medium, Phys. Lett. B **345,** 277 (1995).

[42] R. L. Workman *et al.* (Particle Data Group), Review of particle physics, Prog. Theor. Exp. Phys. **2022**, 083C01 (2022).

[43] S. Peigne and A. V. Smilga, Energy losses in a hot plasma revisited, Phys. Usp. **52**, 659 (2009).

[44] K. Tuchin, Anomalous scattering and transport in chiral matter, Phys. Lett. B **808**, 135680 (2020).

[45] X.-G. Huang and K. Tuchin, Transition radiation as a probe of the chiral anomaly, Phys. Rev. Lett. **121**, 182301 (2018).

[46] K. Tuchin, Chiral Cherenkov and chiral transition radiation in anisotropic matter, Phys. Rev. D **98**, 114026 (2018).

[47] L. D. Landau and I. Pomeranchuk, Limits of applicability of the theory of bremsstrahlung electrons and pair production at high-energies, Dokl. Akad. Nauk Ser. Fiz. **92**, 535 (1953).

[48] A. B. Migdal, Bremsstrahlung and pair production in condensed media at high-energies, Phys. Rev. **103**, 1811 (1956).